Precipitation within Unilamellar Vesicles. Part 1. Studies of Silver(I) Oxide Formation

Stephen Mann * and Robert J. P. Williams
Inorganic Chemistry Laboratory, South Parks Road, Oxford OX1 3QR

The precipitation of small (*ca.* 10 nm) Ag_2O crystallites within unilamellar vesicles has been studied by electron microscopy and light scattering. Many single-domain intravesicular crystallites have been observed by high-resolution imaging, indicating that crystallisation often initiates at a single site on the inner membrane surface followed by slow crystal growth. Under certain experimental conditions no nucleation has been observed below an extravesicular pH (pH_{out}) of *ca.* 11.0 due to negligible diffusion of OH^- across the membrane. Above a pH_{out} of 11.0 the rate of precipitation has been found to be dependent on the rate of crystal growth. Semi-quantitative experiments have shown that the kinetics are first order with respect to intravesicular silver(I) concentration and first order with respect to extravesicular OH^- concentration between a pH_{out} of 11.0 and 12.0. The general possibility of control of precipitation by a vesicle membrane is discussed.

The precipitation of inorganic solids within biological systems is usually achieved by cells having intracellular compartments into which specific elements can be directed. These compartments are often in the form of membrane-bound vesicles and in different cells there are a variety of vesicles ranging in size and function. Many different types of inorganic solids have been located in these vesicles as biomineralised deposits but in general the substances stored are $CaCO_3$ (calcite and aragonite), $Ca_5(OH)PO_4$ (hydroxyapatite), SiO_2 (hydrated silica), and iron oxides (magnetite and lepidocrocite). We wish to investigate not only the types of precipitate which are formed but also the control exerted by the nature of the vesicles since the chemistry of formation of these materials may be very different from the corresponding mass precipitation reactions investigated in inorganic chemistry. First, these biosolids are formed in small confined spaces so that it is the chemistry of a microvolume which must be studied and not the corresponding reaction in free solution. Secondly, precipitation in biological compartments is controlled by many cellular activities and ion transport. Thirdly, ion precipitation in biological systems often occurs through nucleation on organic residues in a matrix of protein and polysaccharide. The resulting crystals or particulates may remain small due to inhibitory effects of the vesicle environment, or may be allowed to grow in particular orientations by cellular control. The resulting morphology may then be very different from that of crystals allowed to grow in free solution. The solids formed may bear little resemblance to their non-biological counterparts since they are intricately sculptured so as to serve some functional use. Thus the formation of biomaterials illustrates the interplay between (inaminate) molecular forces which tend towards a minimum-energy configuration and the organisational capacity of the living cell which generates kinetically stabilised materials.

In order to investigate the chemistry of precipitation in such confined spaces a model system has to be established since an *in vivo* study must be extremely complicated. We have devised a suitable system by carrying out reactions in prepared small (diameter 35—50 nm) unilamellar phosphatidylcholine (pc) vesicles formed by sonicating dispersions of the lipid in aqueous solution at a temperature above the gel-liquid transition point. The advantage of this system is that it has the required two controlled compartments, internal and external phases. Ions can thus be encapsulated in the small internal compartment. By subsequently diffusing suitable ions of opposite charge across the bilayer membrane from the external phase, intravesicular precipitation can be investigated under controlled reaction conditions.

The reaction system chosen for the first study was the precipitation of silver(I) oxide within pc vesicles. The nucleation and kinetics of precipitation of this material within the vesicle microenvironment have been studied by electron microscopy (e.m.) and light scattering. This system was chosen since it was found that high concentrations (*ca.* 250 mmol dm^{-3}) of silver(I) ions could be encapsulated within the vesicles without precipitation of the lipid. Hence intravesicular particulates of different size could be studied. In passing we note that very small homogeneous Ag_2O particles could have important uses in catalysts.

Experimental

Preparation of Silver(I) Oxide within pc Vesicles.—Grade 1 egg yolk pc in chloroform–methanol solution was obtained from Lipid Products. All other chemicals were of AnalaR grade. A volume of the pc solution was evaporated to dryness *in vacuo* using a rotary evaporator with a liquid nitrogen trap. The resulting lipid film was dispersed in $AgNO_3$ solution at pH = 5.0 to give a dispersion 17 mmol dm^{-3} in pc and then sonicated in the dark at 4 °C until the solution was no longer turbid (*ca.* 5—10 min). Very high concentrations of $AgNO_3$ solution, *e.g.* 1 mol dm^{-3}, were avoided since they caused precipitation of the lipid, preventing vesicle formation on sonication. After sonication the opalescent solution was passed down a cation ion-exchange column (Permutit Zeocarb 225, sodium form) to remove the silver(I) ions from the external phase of the vesicles. The pH of the vesicle solution after passage through the column was observed to be in the range 8.0—9.0. No precipitation was apparent at this stage. The vesicle solution was then raised to pH 12.0—12.6 by addition of NaOH solution, whereupon it turned progressively darker with intravesicular Ag_2O precipitation and after *ca.* 10 min was light brown in colour. No precipitation of this solution was observed on centrifugation with a bench centrifuge.

Leaving the vesicle samples in the air at room temperature for 24 h at a pH of 12.3 resulted in the formation of a brown gel indicating the instability of the vesicle–Ag_2O system to hydrolysis over this period.

Electron Microscopy.—For routine investigations a JEOL 100CX TEMSCAN analytical electron microscope was used operating at an accelerating voltage of 100 keV. For ultra-

high-resolution imaging a JEOL 200CX THG2 electron microscope was used operating at 200 keV ($\approx 3.20 \times 10^{-17}$ J) with a high brightness LaB_6 electron source and a point-to-point resolution of 0.246 nm. In the study of vesicles one drop of the above brown vesicle solution was placed on carbon-sputtered, formvar-coated copper e.m. grids and left to dry on filter paper.

Light Scattering.—To measure light scattering a Carey model 17 spectrophotometer operating at a fixed wavelength of 600 nm, slit width 0.2—0.35 nm, was used with 1-cm pathlength cells. All experiments were carried out at room temperature (298 ± 3 K). Light-scattering and pH measurements were made before and after addition of small aliquots (0.05 cm^3) of sodium hydroxide solutions (0.1—1.0 mol dm^{-3}) to the vesicle solutions. The change in turbidity at 600 nm was then followed directly with time. Intravesicular silver(I) concentrations were measured using flame atomic absorption spectroscopy. Concentrations are quoted as moles of Ag^I per litre of solution although all the Ag^I is in the vesicles. A series of lipid solutions (17 mmol dm^{-3} lipid) of known silver(I) concentration were analysed by atomic absorption spectroscopy in order to derive a calibration curve for vesicle samples of unknown silver(I) concentration. The presence of lipid was observed to suppress silver(I) concentrations by 30% relative to those in the absence of lipid.

Results and Discussion

Our initial experiments were concerned with the demonstration that Ag_2O precipitation took place within intact vesicles. The use of intravesicular paramagnetic cobalt(II) ions in place of the silver(I) ions used here had already shown that the general methods described in this paper for the precipitation of inorganic oxides/hydroxides within intact pc vesicles is valid.[1] Observations consistent with this conclusion are as follows. First, the intravesicular Ag_2O particles are essentially homogeneous in size unlike those precipitated under the same conditions in the absence of vesicles where a large range of crystallite diameters have been observed ranging from 10 nm to large aggregates (4 μm). Secondly, precipitation did not occur until pH 11.0 which is four pH units higher than in the absence of vesicles. Thirdly, bench centrifugation of colloidal Ag_2O (no vesicles) resulted in rapid sedimentation but no such sedimentation was observed in the experiments described here. Finally, *X*-ray microprobe analysis showed that Ag_2O precipitation occurred within volumes associated with the phosphorus of lipids, *i.e.* of vesicles.

The vesicles containing precipitated Ag_2O were seen as discrete electron-dense spheres in the 100CX electron microscope (Figure 1). The sizes of one hundred particles were measured. The range of particle size is extremely small as shown by the frequency distribution curve in Figure 2. Only the area enclosed by the Ag_2O particulates could be observed; the lipid membrane is not imaged due to the low contrast (small degree of electron scattering) of its constituent atoms. The arithmetic mean diameter was 10.55 nm with a standard deviation of population of 1.25 nm. This degree of homogeneity may be expected since the sonication method of vesicle preparation forms vesicles of uniform size.[2] Vesicles prepared by this method were found to be 30—60 nm in diameter when investigated in the electron microscope after negative staining with uranyl acetate. Calculations based on an intravesicular silver(I) concentration of 250 mmol dm^{-3} within a vesicle of diameter 50 nm predicted that the resulting particle diameter would be *ca.* 8 nm. Since larger particulates could sometimes be observed of diameter *ca.* 50 nm, there may

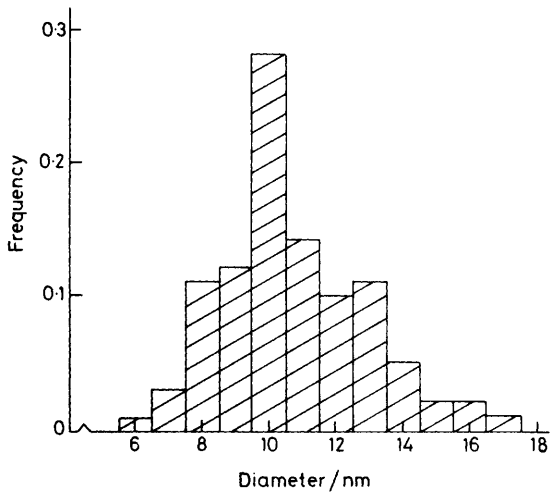

Figure 2. Frequency distribution diagram for intravesicular Ag_2O particulates formed from a sonicated solution of 250 mmol dm^{-3} silver(I) ions

be larger vesicles (liposomes) or some vesicle fusion occurring within the sonicated sample.

X-Ray electron microprobe analysis was performed over areas of the particles in order to identify the elements present in these regions of space. The smallest area analysed was 30 × 30 nm since it was not possible to analyse a single particle. Analysis was generally performed for 100 s at a tilt angle of 40°. Dense regions of particles such as in Figure 1 gave well resolved *X*-ray peaks above background (Figure 3) revealing the presence of phosphorus (P) (from the phospholipid) and silver (Ag) only in these regions. (Copper peaks originate from the e.m. grid.) *X*-Ray microprobe analysis in regions away from the particulates did not detect P or Ag.

Electron diffraction was performed over areas of the Ag_2O particles and powder-diffraction images were observed. Thus the intravesicular Ag_2O formed is crystalline. *d* Spacings were calculated in nm and then compared with reference standards for cubic [3] and hexagonal [4] Ag_2O, and with similar measurements made for a Ag_2O sample prepared similarly in distilled water without the presence of lipid (Table). The results showed that the intravesicular Ag_2O had the same crystal morphology as the Ag_2O prepared in distilled water in the absence of lipid. Comparison of the *d* spacings of the lines for Ag_2O (intravesicular) with reference standards indicated that the intravesicular crystallites were cubic in structure.

Intravesicular Ag_2O particles imaged at high resolution showed the crystallites to be mostly single-domain crystallites although some multi-domain crystallites were also observed. Figure 4 shows lattice fringes corresponding to the 111 plane running across a Ag_2O crystallite with the edge of the particle towards the top of the figure. The 111 lattice plane is also the strongest *d* spacing observed in the electron-diffraction pattern of intravesicular Ag_2O. Lattice spacings could be resolved on particulates down to 6 nm in diameter; for particulates below this size no spacings could be imaged.

The formation of single- and multi-domain crystallites indicates that nucleation occurs at only a few sites in the vesicle. Nucleation within vesicles is expected to be homogeneous in the sense that the vesicle volume is so small that the probability of there being a foreign particle in the vesicular space is very low, but heterogeneous in the sense that there is a lipid surface on which nucleation may initiate. Silver(I) ions will be located close to the membrane under the influence of the negatively charged phosphate headgroups. The membrane

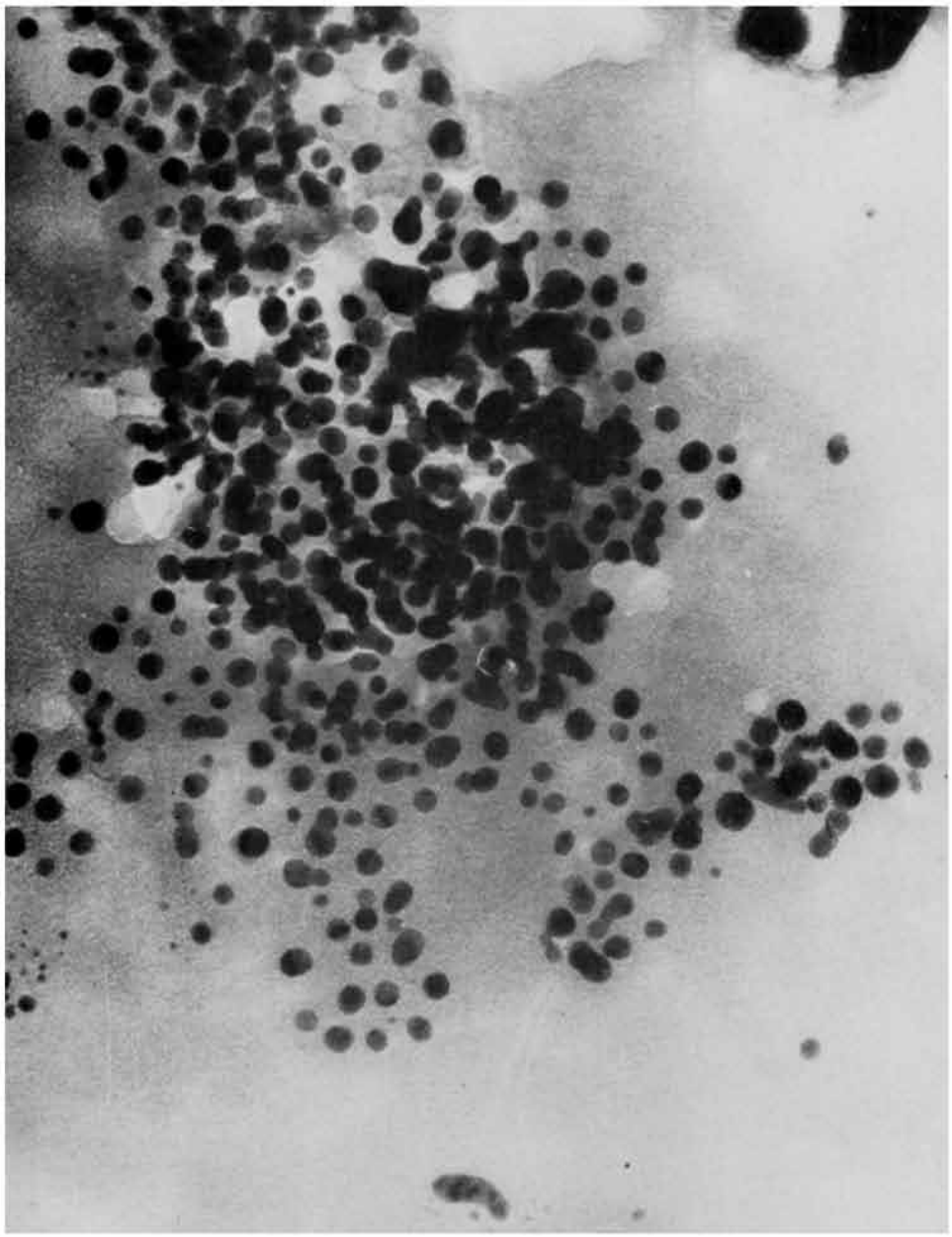

Figure 1. Electron micrograph of intravesicular Ag_2O particulates $\times 286\,000$

To face page 312

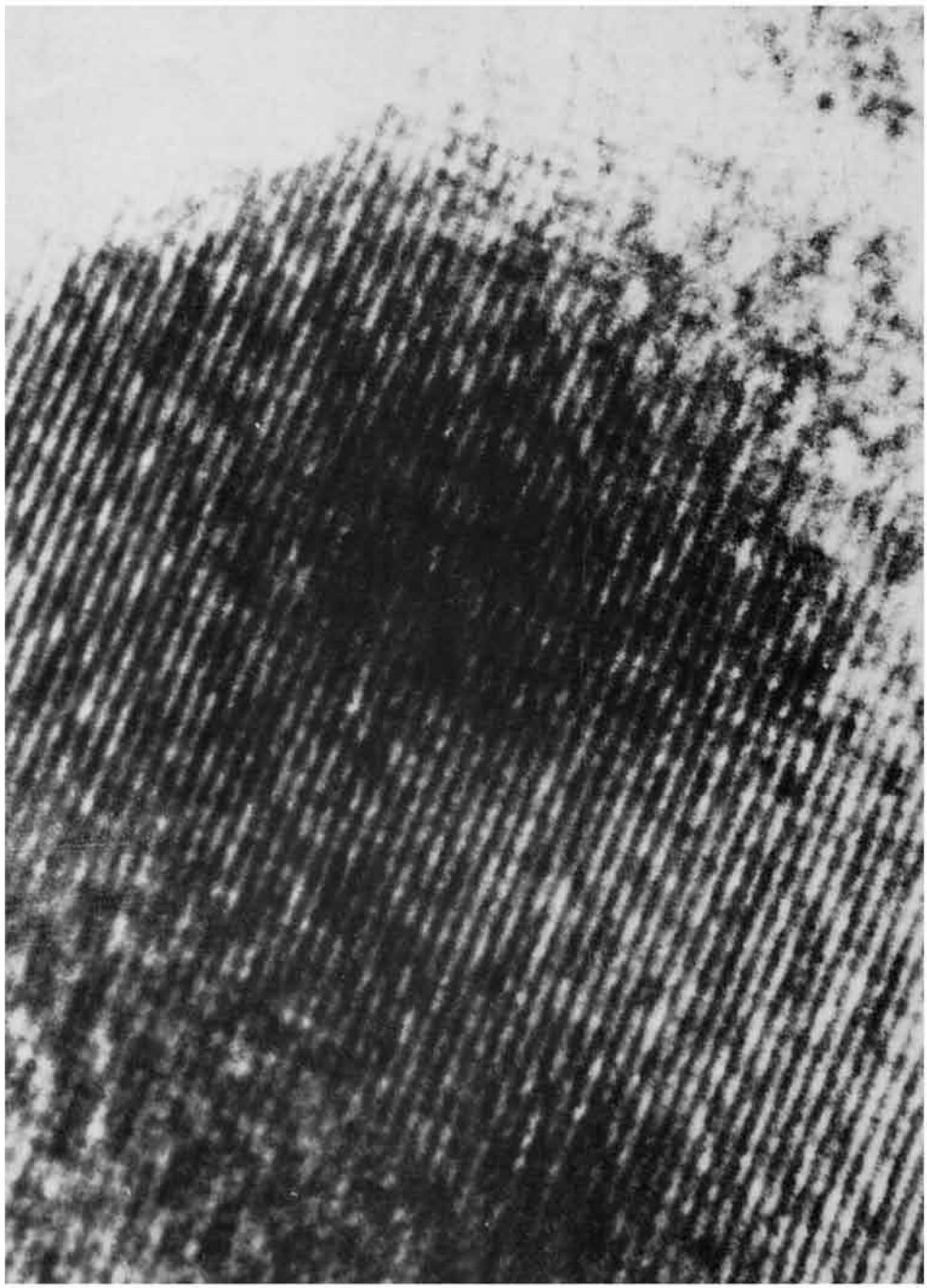

Figure 4. Ultra-high-resolution electron micrograph showing lattice fringes across an intravesicular Ag_2O crystallite $\times 9\,800\,000$

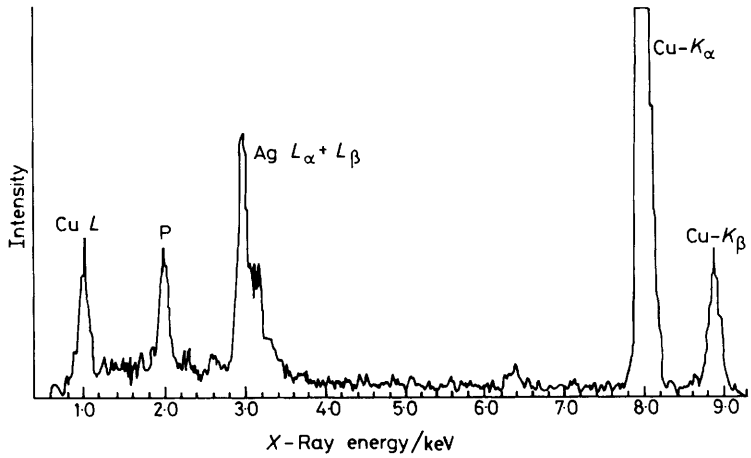

Figure 3. *X*-Ray microprobe analysis of intravesicular Ag_2O particulates

Table. Powder-diffraction data (*d* spacings in nm) for various Ag_2O samples; s = strong intensity. Estimated error on experimental data, ±5%

Ag_2O (distilled water)	Ag_2O (intravesicular)	Ag_2O (cubic *)	Ag_2O (hexagonal *)
0.306		0.335	
0.265(s)	0.268(s)	0.273(s)	0.264
0.222(s)	0.228(s)	0.237(s)	0.233(s)
			0.181(s)
0.164	0.164(s)	0.167(s)	0.164
			0.153
0.141	0.141(s)	0.143(s)	0.140(s)
			0.130(s)
0.111	0.104	0.106	

* Reference standard (see text).

is not absolutely homogeneous of course since some lecithin is inevitably hydrolysed and there may be a suitable site on the membrane acting as a nucleation centre. Once nucleation has begun and the critical nucleus size surpassed then this site will be more favourable than any other site for single crystals to develop. If nucleation had occurred simultaneously at many headgroup sites an annulus of material would have been expected to form around the vesicle membrane possibly preventing further reaction (Figure 5). Intravesicular Ag_2O crystallites imaged after 10 s of reaction showed discrete, often angular particles which supports an essentially single site model of nucleation. By contrast cobalt(II) ions precipitated as hydroxide in vesicles resulted in halo-like e.m. images which corresponded to the initial stages of amorphous $Co(OH)_2$ precipitation indicating that nucleation occurred simultaneously at many sites on the inner membrane surface.[5] Figure 5 illustrates possible mechanisms of Ag_2O nucleation within the vesicles.

Light scattering was used next to study semi-quantitatively the kinetics of intravesicular Ag_2O formation. The theory of light scattering has been extensively studied.[6,7] For large particle sizes the theory is complex but for particles of radius $<\lambda/10$, where λ is the wavelength of the light scattered, the theory is relatively simple and obeys the Rayleigh condition (1), where τ = turbidity, measured by optical density (absorbance), K = a constant dependent on the refractive indices of solute and solvent, r = particle radius, and N = number of particles per unit volume. For a spherical particle, volume V is proportional to r^3 and equation (1) can be rewritten as (2).

$$\tau = Kr^6N/\lambda^4 \quad (1)$$

$$\tau = K'V^2N/\lambda^4 \quad (2)$$

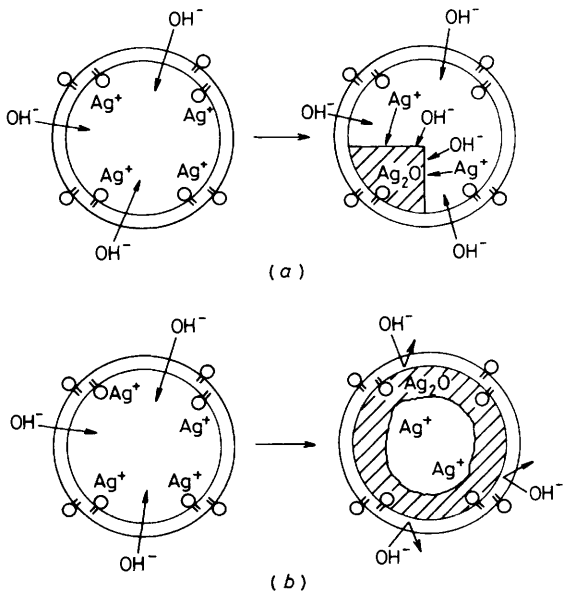

Figure 5. Possible mechanisms of Ag_2O nucleation within vesicles: (*a*), nucleation at a single site; (*b*), nucleation at several sites along the vesicle membrane

Eight vesicle samples (17 mmol dm^{-3} in lipid) were prepared incorporating different silver(I) concentrations within the internal vesicle volume. For each vesicle sample the pH was raised to 12.3 using sodium hydroxide solutions and the increase in turbidity at 600 nm (τ_{600}) measured with time. Figure 6, curves (*b*)—(*d*), shows the changes in turbidity at 600 nm for different internal silver(I) concentrations. The formation of intravesicular Ag_2O is slow as shown from the slope of the curves. For Ag_2O precipitation in normal aqueous solution (no vesicles) the resulting turbidity change is instantaneous. The curve for vesicles prepared in the absence of silver(I) ions [curve (*a*), ' blank ' vesicles] shows a characteristic small (0.01) initial rise in turbidity after sodium hydroxide addition followed by a decrease in light scattered back to its

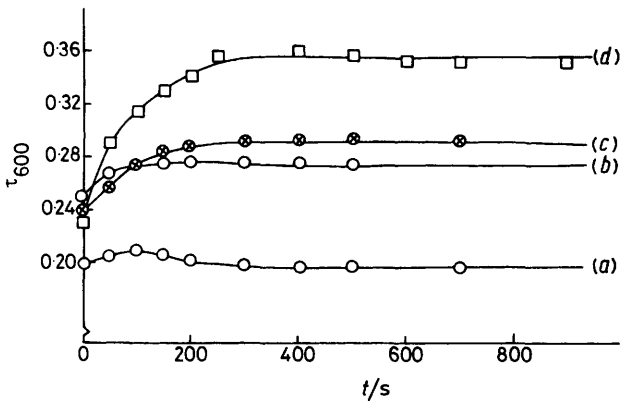

Figure 6. Change in turbidity at 600 nm ($\tau_{600} \pm 0.003$) with time after the addition of NaOH (aq) to a final pH value of 12.3 for vesicle solutions containing different internal silver(I) concentrations: (*a*), ' blank ' vesicles; (*b*), 5.1 $\times 10^{-5}$ mol dm^{-3}; (*c*), 17.2 $\times$ 10^{-5} mol dm^{-3}; (*d*), 33.8 $\times$ 10^{-5} mol dm^{-3}

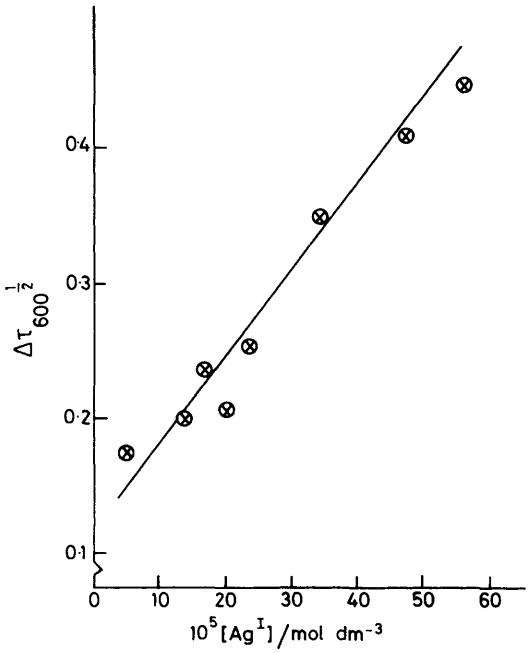

Figure 7. Relationship between the square root of the total turbidity change at 600 nm ($\Delta\tau_{600}^{\frac{1}{2}} \pm 0.01$) and the intravesicular silver(I) concentration (final pH = 12.3) indicating that the Rayleigh condition holds for intravesicular precipitation

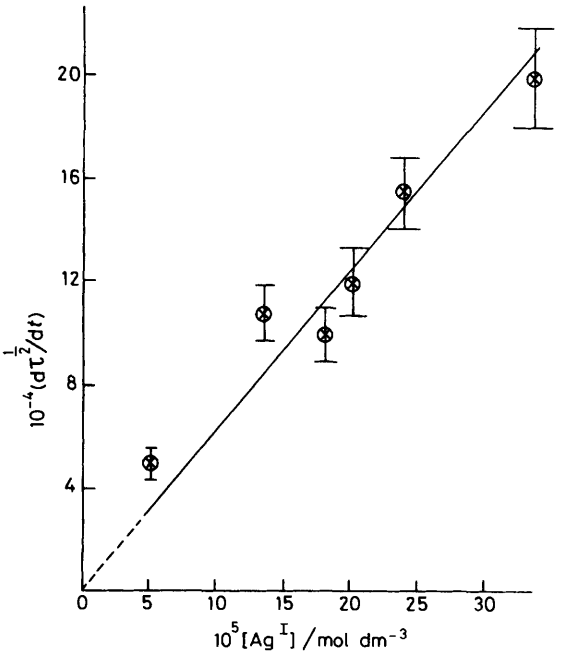

Figure 8. Plot of initial rate of precipitation ($d\tau^{\frac{1}{2}}/dt$, estimated error $\pm 10\%$) against initial intravesicular silver(I) concentration (estimated error $\pm 5\%$) for a final pH = 12.3

original value. No further change in turbidity at pH 12.3 is observed over 3.5 h which indicates that the vesicles are stable at high pH over this period.

The Rayleigh condition of light scattering was studied by plotting the square root of the total increase in turbidity ($\Delta\tau_{600}^{\frac{1}{2}}$), calculated from graphs as in Figure 6, against the concentration of intravesicular silver(I) ions expressed in moles per litre of vesicle solution. From equation (2), for vesicle solutions of constant concentration in lipid and assuming that nucleation occurs in each vesicle, the total turbidity change is proportional to the square of the particle volume and for a reaction going to completion is proportional to the square of the initial intravesicular silver(I) concentration $[Ag^I]_{in}$ for particles of constant density. Figure 7 shows a linear relationship between $\Delta\tau_{600}^{\frac{1}{2}}$ and intravesicular silver(I) concentration indicating that Rayleigh scattering is observed under these experimental conditions.

The $[Ag^I]_{in}$ dependence of the initial precipitation rate was determined by measuring the initial slope of curves such as those in Figure 6 since in each case the final extravesicular pH was the same. The corresponding plot of these gradients against initial intravesicular silver(I) concentration is shown in Figure 8. The graph reveals a linear relationship between the initial rate of precipitation and trapped silver(I) concentration at constant hydroxide-ion concentration. Thus over the concentration range investigated the initial kinetics are first order with respect to $[Ag^I]_{in}$.

The hydroxide-ion dependence of the initial intravesicular precipitation rate was determined by measuring the initial slopes of turbidity curves using vesicles containing the same $[Ag^I]_{in}$ but with the final extravesicular pH raised to different values. Figure 9 shows the change in turbidity with time for five different final pH values for vesicles containing an initial $[Ag^I]_{in}$ of 20.3 $\times$ 10^{-5} mol dm^{-3}. Addition of OH^- to give a final extravesicular pH less than 10.8 resulted in no observable increase in turbidity. In fact a slight fall in turbidity was noted due to dilution effects. Thus no Ag_2O formation was observed below this pH value. At intermediate pH (11.0—12.0) an increase in turbidity was observed after an induction period of *ca.* 20 s implying that the reaction proceeds but is slow over this pH range. At high pH (12.0—12.6) the increase in turbidity followed a similar pattern as observed in Figure 6. A plot of initial rate against initial hydroxide-ion concentration is shown in Figure 10. At pH values below 12.0 the initial rate of precipitation was observed to be strongly dependent on extravesicular pH, $[OH^-]_{out}$. Above this pH the initial rate became less dependent on change of $[OH^-]_{out}$.

These kinetic results are only semi-quantitative since there are many possible errors in the light-scattering method of following precipitation reactions. Thus in Figure 7 the reason the graph does not pass through the origin is most probably due

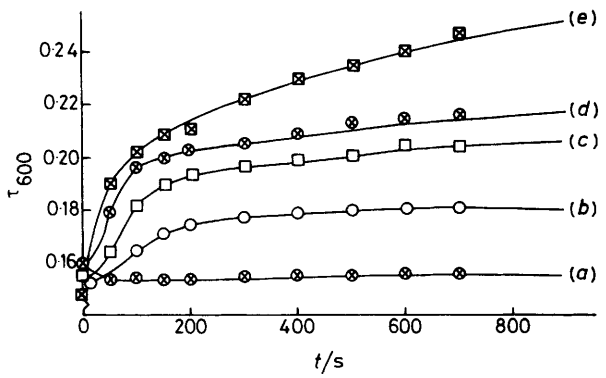

Figure 9. Change in turbidity ($\tau_{600} \pm 0.004$) with time for Ag^I-containing vesicles (20.3×10^{-5} mol dm^{-3}) after the addition of NaOH (aq) ($t = 0$) to give different pH values: (*a*), 10.8; (*b*), 11.5; (*c*), 11.95; (*d*), 12.3; (*e*), 12.6

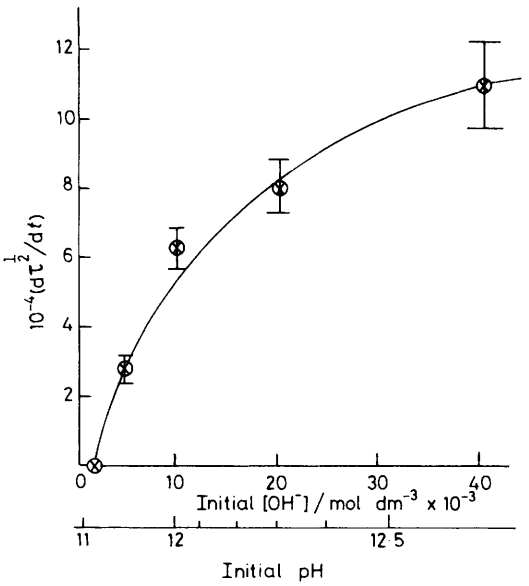

Figure 10. Plot of initial rate of precipitation ($d\tau^{\frac{1}{2}}/dt$, estimated error $\pm 10\%$) against OH^- concentration (pH_{out}, estimated error $\pm 5\%$) for Ag^I-containing vesicles (20.3×10^{-5} mol dm^{-3})

to some absorption of the light by the brown Ag_2O particles. There will be other errors in the turbidity measurements particularly since the particle volume is assumed constant at any given time which will only be partially true since there is a range of vesicle sizes. Also, dilution factors were not considered in the calculation of initial rates.

There are at least two possible steps in the reaction mechanism of Ag_2O formation within pc vesicles [equations (3) and (4)]. The first step is diffusion controlled and depends on the

$$OH^-(aq)_{out} \xrightarrow{k_{diff}} OH^-(aq)_{in} \quad (3)$$

$$2OH^-(aq)_{in} + 2Ag^+(aq)_{in} \xrightarrow{k} Ag_2O(s)_{in} + H_2O \quad (4)$$

rate of passage of OH^- ions through the lipid membrane. The diffusion rate of many anions is known to be *ca.* 10^5 times faster than for cations which have very low permeabilities across lipid membranes.[8] Thus the possibility of increasing intravesicular pH by efflux of H^+ is not considered.

The turbidity curves presented for intravesicular Ag_2O precipitation (Figures 6 and 9) show that crystallisation begins almost immediately and then continues at a slow rate. This is in agreement with the rate of precipitation being dependent on the rate of crystal growth and not on the rate of nucleation. If the rate of nucleation had been the limiting process, turbidity would have risen sharply over a short time range after which precipitation would have been essentially complete.

In general, the kinetic behaviour of intravesicular Ag_2O precipitation can be expressed therefore as in equation (5) or at time t as in (6) where K_{sp} is the solubility product for Ag_2O

$$\text{rate of precipitation} = \text{rate of crystal growth} = R$$

$$R = K(\text{supersaturation})^x \quad (5)$$

$$R_t = K[Ag^I]_{in,t}[OH^-]^z_{in,t} - K_{sp} \quad (6)$$

and activities rather than concentrations are applicable. Our experiments, although only semi-quantitative, show that under the experimental conditions considered the observed rate is first order with respect to both $[OH^-]_{out}$ (between pH 11.0 and 12.0) and $[Ag^I]_{in}$. Thus for vesicles containing the same $[Ag^I]_{in}$ but raised to different steady-state pH_{in} values we obtain expression (7). Here $J_{OH,t}$ = hydroxide net flux at time

$$R_t = k[OH^-]_{in,t} \quad (7)$$

where

$$[OH^-]_{in,t} = \left([OH^-]_{in,t=0} + \int_0^t J_{OH^-,t}\,dt\right) - [OH^-]_{crystal,t}$$

t. The relationship between $[OH^-]_{in,t}$ and $[OH^-]_{out,t}$ is discussed elsewhere.[1] Thus supersaturation in the vesicles will be dependent on the initial $[Ag^I]_{in}$ and the rate of hydroxide diffusion across the membrane, *i.e.* pH_{out}.

At pH_{out} values below 11.0 the rate of OH^- influx is very small and supersaturation is never attained within the vesicles (for a $[Ag^I]_{in}$ of 100 mmol dm^{-3} an intravesicular pH of *ca.* 7.0 is required for precipitation). At pH_{out} values above 12.0 the rate of crystal growth becomes less dependent on initial pH gradients across the membrane which suggests that there is a limiting maximum rate of diffusion through the membrane such that the rate of increase of pH inside the vesicles is no longer determined by changes in the external $[OH^-]$.

In general the rate of nucleation will be a function of the supersaturation since aggregates of ions are formed by statistical fluctuations in the solution and so the probability of a cluster of Ag^+ and OH^- ions exceeding the critical nucleus required for continued crystal growth will be higher at larger intravesicular supersaturation values. Thus the low levels of supersaturation maintained by the slow rate of OH^- influx favour only a few sites for nucleation within the vesicle followed by controlled growth of well defined crystallites. Crystal growth will then occur through the advancement of steps on different crystal faces *via* surface nucleation and screw dislocations in the developing crystallite.[9]

The dependency of the rate at which supersaturation is maintained within the vesicles on anion diffusion rates is clearly revealed when anions of different permeabilities are substituted for OH^- and the corresponding intravesicular precipitation followed by turbidity measurements. Figure 11 shows the change in turbidity for the same concentration of intravesicular Ag^I after addition of different anions. Graph (*a*) is for AgCl formation, (*b*) is for Ag_2O precipitation as described above, and (*c*) is for Ag_2S precipitation. In the case of intravesicular AgCl formation the increase in turbidity with time due to the addition of Cl^- is much slower than for Ag_2O formation indicating that diffusion of Cl^- across the lipid

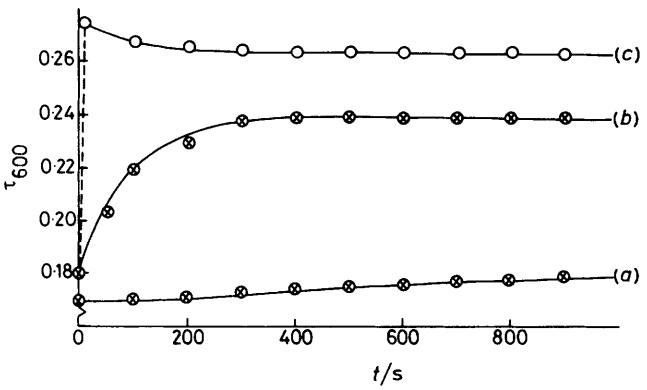

Figure 11. Turbidity curves for (*a*) AgCl, (*b*) Ag_2O, and (*c*) Ag_2S formation within vesicles containing the same concentration of silver(I) ions (20.3×10^{-5} mol dm^{-3})

membrane is much slower than that of OH^-. In (*c*) the formation of intravesicular Ag_2S occurs instantaneously after the addition of $(NH_4)_2S$. The turbidity of this sample rises immediately from 0.178 to 0.275. This is due to the rapid diffusion across the vesicle membrane of free molecular H_2S in the $(NH_4)_2S$ solution. There is a slight decrease in turbidity with time before reaching a steady turbidity value which seems to indicate that the particulates formed initially are in non-equilibrium conditions and come to equilibrium within 150 s of formation. The final turbidity values for intravesicular Ag_2S, Ag_2O, and AgCl formation will be different depending on the refractive indices of the different particulates formed.

The processes occurring in the formation of intravesicular Ag_2O are related closely to one possible mechanism of biomineralisation, namely the inclusion of a cation and its adsorption onto an organic matrix followed by precipitation. Thus nucleation and particulate growth studies using the vesicle system provide an excellent model for mineralisation in biological compartments.

Further kinetic/nucleation experiments concerning intravesicular Ag_2O precipitation could involve the incorporation of inhibitors such as long-chain carboxylates or phosphonates in the vesicle membrane. The effect of these molecules on crystallisation could then be studied by ultra-high resolution e.m. The use of such techniques would also make it possible to study the nature of defects in crystallites prepared within vesicles.

One important conclusion from this work is the use of the lipid membrane in controlling intravesicular precipitation under certain experimental conditions. Such processes are critical in biological systems. The measurement of intravesicular pH with changes in extravesicular pH under reaction conditions similar to those discussed in this paper can be studied by ^{31}P n.m.r. spectroscopy and will be described in a subsequent publication.[1]

Acknowledgements

We thank Dr. A. J. Skarnulis for assistance with electron microscopy and Mr. J. Kench for flame atomic absorption measurements.

References

1 S. Mann, M. J. Kime, R. G. Ratcliffe, and R. J. P. Williams, *J. Chem. Soc., Dalton Trans.*, 1983, in the press
2 C. Huang, *Biochemistry*, 1969, **8**, 344.
3 ASTM Powder Diffraction File 1972, 12–793.
4 ASTM Powder Diffraction File 1972, 19–1155.
5 S. Mann, D.Phil. Thesis, Oxford, 1982.
6 Lord Rayleigh, *Philos. Mag.*, 1899, **47**, 375.
7 G. Mie, *Ann. Phys. (Leipzig)*, 1908, **25**, 377.
8 A. D. Bangham, *Protoplasma*, 1967, **63**, 183.
9 W. K. Burton, N. Caberra, and F. C. Frank, *Philos. Trans. R. Soc., London, Ser. A*, 1951, **243**, 299.

Received 28*th April* 1982; *Paper* 2/698